

Absolute cross section for the photodisintegration of deuterium

Y. Birenbaum, S. Kahane, and R. Moreh

Nuclear Research Center—Negev, Beer-Sheva, Israel
and Ben-Gurion University of the Negev, Beer-Sheva, Israel

(Received 11 February 1985)

Accurate absolute cross sections for the photodisintegration of deuterium were experimentally determined, using an absorption method, at the following photon energies: 5.97, 7.25, 7.60, 7.64, 8.80, 9.00, and 11.39 MeV with uncertainties generally less than 3%. The photon beams were produced by thermal neutron capture, and the absorption through 2 m absorbers of H₂O and D₂O was measured. The results are in excellent agreement with theoretical predictions with a preference for calculations using soft core potentials and including explicitly the effects of meson-exchange currents.

I. INTRODUCTION

In the past, several measurements of the absolute cross section for the photodisintegration of deuterium were carried out. The corresponding data have been compiled at the National Bureau of Standards,¹ and a critical review of the results in the 10–120 MeV range is given in Ref. 2. At $E < 12$ MeV most of the measurements were done in the 1950's.^{3–5} The results were of poor accuracy and usually employed photons obtained from radioactive sources. Further, the data (with the exception of those of Ref. 5) largely deviate from present theoretical predictions.^{6,7} In a more recent work⁸ published in 1972, using $E < 12$ MeV, the results were of limited accuracy (25%) and were obtained primarily for testing the experimental system. A comparison between previous experimental results and theory is presented in Fig. 1. The three lines correspond to different theoretical calculations as will be discussed

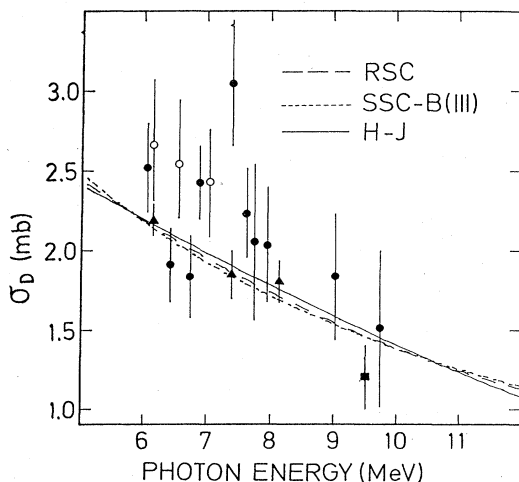


FIG. 1. Previously measured absolute photodisintegration cross sections. Closed circles are taken from Ref. 8, open circles from Ref. 4, triangles from Ref. 5, the square from Ref. 3. The solid, dashed, and dotted lines are defined in the caption to Fig. 4.

fully in Sec. IV. At $E > 12$ MeV, the experimental results of Ahrens *et al.* (with an accuracy of 5%) disagreed with earlier data^{10,11} and showed good agreement with theory.

In the present work, we report the results of a new cross section measurement at seven photon energies in the range of 6–11.4 MeV with an accuracy generally better than 3%. The results are in very good agreement with present theoretical predictions.^{6,7} Two factors contributed to the high accuracy achieved in the present work. First, an absorption method was used which is free of the errors involved in absolute photon beam intensity measurements. Second, the available beam intensities were very high, enabling the accumulation of very good statistics in a reasonable length of time.

II. EXPERIMENTAL PROCEDURE

A. Photon beams

The experimental system is illustrated in Fig. 2. The photon beams were generated from the (n, γ) reaction on metallic disks of Fe and Ni placed along a tangential beam tube and near the core of the IRR-2 reactor.¹³ For each γ source about six disks, 2 cm thick and 7 cm in diameter, were used. The Fe disks were used for generating the 7.64, 7.60, 7.25, and 5.97 MeV photons (consisting of the 5.92 + 6.02 MeV γ lines¹⁴). The Ni disks generated the 8.80, 9.00, and 11.39 MeV photons. The latter line does not occur in the $^{58}\text{Ni}(n, \gamma)$ spectrum and is produced through successive neutron capture on the naturally occurring ^{58}Ni isotope, namely through the $^{58}\text{Ni}(n, \gamma)^{59}\text{Ni}(n, \gamma)$ process.¹⁵ The photon energies of 7.25, 7.60, and 8.80 MeV do not correspond to actual lines emitted by the γ sources but rather to weighted average energies as explained in Sec. III. The photon beam obtained was collimated and neutron filtered by passing it through 40 cm of borated paraffin. The resulting intensities of the γ lines were of the order of 10^6 photons/cm² sec at the position of the absorber. The absolute photodisintegration cross section was measured by comparing the transmitted photon intensities after passing the photon beam through equivalent length of two absorbers (~ 2 m) consisting of light water (H₂O) and heavy water (D₂O). The transmit-

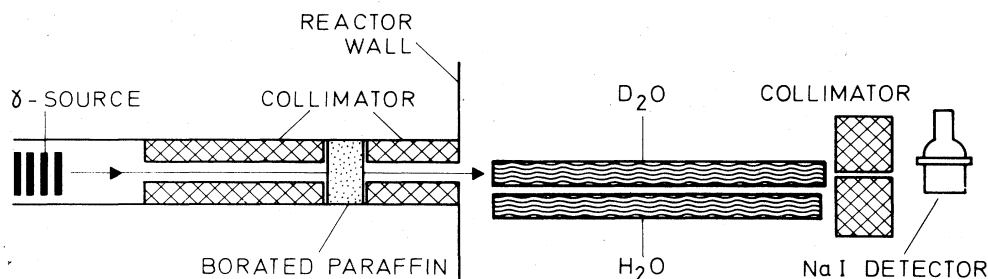


FIG. 2. Schematic diagram (not to scale) of the experimental system showing γ source, collimators, D_2O and H_2O absorbers, and the detector.

ted photons were detected using a 7.6×7.6 cm NaI crystal. It may be noted that the resulting beam intensity, after passing through the 2 m long water absorbers, was much higher than could be tolerated by the electronics of our counting system. It was thus necessary to attenuate the incident beam in order to keep the pileup corrections to very low levels.

B. Absorbers

The absorbers consisted of stainless steel tubes of equal internal dimensions (4.2 cm) and different lengths: ~ 199.3 cm (filled with H_2O) and ~ 200 cm (filled with D_2O). The ends of the tubes were sealed with thin plates of equal thickness (0.5 mm). The length of the absorbers were chosen to satisfy the relation

$$l_H/l_D = V_H/V_D, \quad (1)$$

where l_H, l_D and V_H, V_D represent the lengths and molar volumes of the absorbers. With this choice the atomic attenuation of the photons in the two tubes becomes identical, and the difference in the transmitted intensities, which varies between 1.5% and 2.7% over the range of our photon energies, is entirely due to nuclear absorption via the $^2H(\gamma, n)$ reaction. Actually, the equality of Eq. (1) was achieved only to within four parts in 10^4 and a very weak dependence on the atomic absorption cross section still persisted. The purity and density of the two absorbers were measured. The results, together with some other characteristics of the absorbers, are listed in Table I. The uncertainties appearing in this table produce a $\sim 0.2\%$ uncertainty in the value of σ_D .

It may be noted that a difference between the atomic attenuation cross sections of the D_2O and H_2O absorbers may arise because of a possible difference in the pair pro-

duction by the oxygen nucleus caused by different screening arising from a difference in molar volumes. This difference may be neglected at $E < 11$ MeV as it was estimated by Ahrens *et al.*⁹ in the 15–25 MeV range and found to be $2 \mu b$ for 15 MeV photons and decreasing toward lower energies. The effect of small temperature differences between the two absorbers was also considered because it may change the absorber density and hence the photon attenuation. Such variations were measured over several day periods and were found to be $\pm 0.25^\circ C$ and hence have a negligible effect on the photon attenuation. The effect of multiple scattering along the water absorbers was calculated and found to be negligible because of the small angular aperture subtended by the detector ($\theta \sim 0.6^\circ$).

C. Experimental method

The absorbers were mounted on a sliding table and were positioned to be parallel to each other so that each could be precisely aligned coaxially with the collimators and the photon beam. This was done by photographing the profile of the beam at three points along its path using a polaroid film backed by a lead scatterer. In addition, the dimensions of the collimator facing the absorber and that placed in front of the detector were so adjusted that no scattered radiation from the stainless steel tubes containing the absorbers could reach the NaI detector.

The signals from the NaI crystal were fed to a Canberra multichannel analyzer. The measurement was done using an automatic control system which performed the following sequence of events: (i) The transmitted photon spectrum passing through the H_2O absorber was recorded for a preset time $T_0 = 5$ min in one part of the analyzer memory. (ii) The sliding table was moved to bring the D_2O absorber in position and the γ spectrum was recorded in a second part of the analyzer memory for the same length of time T_0 . At the end of T_0 , the table was moved back bringing the H_2O absorber in the beam position, and the cycle was repeated. In this manner, the variations of the incident photon intensity and the effects of electronic drifts were averaged out and could be considered the same for the two absorbers. Typically an integrated number of 10^6 counts was collected per peak in each run and the intensity ratio determined from the two spectra. About ten such runs were carried out, and the final intensity ratio (Table II) is the weighted average of the separate results.

TABLE I. Characteristics of the absorbers. The numbers in parentheses are the uncertainties in the last digit.

	D_2O	H_2O
Length (cm)	199.967(2) ^a	199.300(2) ^a
Molar volume (cm ³)	18.128 63(36)	18.061 80(36)
Temperature ($^\circ C$)	23.50(25)	23.50(25)
D_2 in absorbers (%)	99.778(2)	0.0148(2)
^{18}O in absorbers (%)	0.38(2)	0.204(2)

^aMeasured with a micrometer.

TABLE II. Ratios I_H/I_D of transmitted photon intensities through the H_2O and D_2O absorbers, and the deduced total photodisintegration cross section σ_D of the deuteron. The errors are standard deviations.

Energy (MeV)	Ratio I_H/I_D	σ_D (10^{-6} b)
5.97	1.0270 \pm 0.0013	2162 \pm 99
7.25 \pm 0.01	1.02334 \pm 0.00011	1882 \pm 11
7.60 \pm 0.01	1.02230 \pm 0.00022	1803 \pm 16
7.64	1.02241 \pm 0.00035	1810 \pm 28
8.80 \pm 0.02	1.01949 \pm 0.00011	1586 \pm 11
9.00	1.01929 \pm 0.00046	1570 \pm 36
11.39	1.01522 \pm 0.00046	1257 \pm 36

The total running time for each absorber was about one week and depended on the γ -line intensity and the "background" in the vicinity of the particular γ line.

D. Preliminary tests

A preliminary series of tests was carried out before the actual measurements.

(a) The effect of pileup was investigated by attenuating the incident photon beam with Fe absorbers of varying length. An 18 cm long absorber was necessary to reduce pileup effects to a negligible level. This is a very important factor because σ_D is small (~ 1.8 mb at 8 MeV) and hence small differences in pileup due to the $\sim 2\%$ larger counting rate with the H_2O absorber could lead to systematically larger values for σ_D .

(b) The parallelism of the two absorbers was tested by repeating the absorption measurements after interchanging the position of the two absorbers. No measurable difference was found between the two situations.

(c) The reliability of the experimental setup was verified by measuring the total atomic absorption cross section in H_2O . This was done by filling both tubes with H_2O and measuring the transmitted intensities through the two absorbers which differ in length by 6.7 mm. The atomic cross section of H_2O obtained for the 9.00 and 11.39 MeV lines were, respectively, 675 ± 7 and 617 ± 12 mb which agree within one standard deviation with the calculated cross sections reported by Hubble,¹⁶ namely, 692 ± 14 and 633 ± 12 mb.

III. RESULTS

A. The Ni γ source

A typical spectrum is given in Fig. 3 which shows the various γ lines. The contribution of the 11.39 MeV line was relatively pure and was calculated by considering the areas of the photopeak and first escape peak. The contribution of the 9.00 MeV line was evaluated from the area of the photopeak only, after subtracting the background effects of the higher energy lines at 10.05 and 11.39 MeV. The 8.53 MeV photopeak and single escape peak contained a strong contribution from the 9.00 MeV single and double escape peaks and also contributions from the photopeaks of the 7.82 and 8.12 MeV lines of the Ni(n,γ)

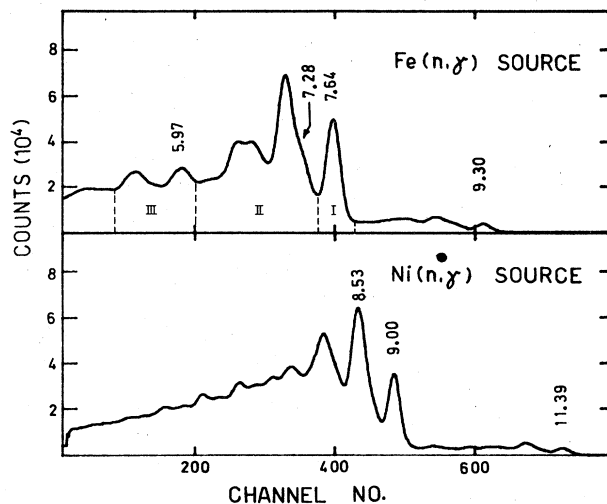


FIG. 3. Transmitted gamma spectrum of the iron and nickel sources as measured using a 7.6 cm \times 7.6 cm NaI detector. The energies (in MeV) of only the photopeaks of the various lines are indicated. The region of the 8.53 MeV peaks of the Ni(n,γ) source contains contributions from γ lines at 9.00, 8.12, and 7.82 MeV. The 7.64 MeV peak of the Fe(n,γ) source consists of two lines at 7.632 and 7.646 MeV, and the 5.97 MeV consist of lines at 5.920 and 6.018 MeV.

spectrum. These four contributions were found to correspond to an average weighted energy of 8.80 ± 0.02 MeV. In calculating the weighted average energy, the relative intensities of the various γ lines, the response function of the NaI detector, and the variation of photodisintegration cross section with energy¹² were accounted for. Here again the background effects of higher energy lines were subtracted.

B. The Fe γ source

The corresponding γ spectrum is shown in Fig. 3 where the γ rays at 7.64 MeV consist of a doublet¹⁴ at 7.632 and 7.646 MeV. Because of the overlapping contributions of the various γ lines, the energy region $E < 7.64$ MeV was divided into three parts as indicated in the figure, and the intensity ratio was deduced from the integrated counts in each region. Thus, the intensity ratio at 7.64 MeV was obtained from the number of counts in the photopeak only. The second energy region (II) includes a major contribution from the single and double escape peaks of the 7.64 MeV together with contribution from the photopeak, single, and double escape peaks of the 7.28 MeV line. These contributions were found to correspond to a weighted average energy of 7.60 ± 0.01 MeV. The third energy region (III in Fig. 3) at and below 5.97 MeV involves major contributions (80%) from the 7.64 and 7.28 MeV photons and only 20% from actual 5.97 MeV photons. The corresponding average weighted energy was 7.25 ± 0.01 MeV. At 5.97 MeV the transmitted intensity ratio was evaluated from region (III) after subtracting the 80% background contributed by the higher energy lines. The relative contributions were obtained from a measurement of the response function of the NaI detector and from a

knowledge of the γ line intensities in the incident photon beam. No intensity ratio was extracted from the 9.30 MeV γ line because of its low statistics and the overlapping effect of the 8.89 MeV γ line.

C. Absolute cross sections

The deuterium photodisintegration cross section, σ_D , was obtained from the theoretical intensity ratio given by

$$R = I_D/I_H = \exp\{N_0\sigma_t[(I_H/V_H) - (I_D/V_D)] - 2N_0(1-\alpha)I_D\sigma_D/V_D\}. \quad (2)$$

N_0 is Avogadro's number, σ_t is the total atomic cross section, and α is the isotopic ratio of H/D in the D_2O absorber. In Eq. (2) the contribution of the photonuclear cross section of the oxygen isotopes is either very small or zero and was ignored.¹ The measured intensity ratios I_H/I_D and the deuterium photodisintegration cross section results are listed in Table II and shown in graphical form in Fig. 4.

IV. DISCUSSION

The cross sections obtained in the present measurement were compared to theoretical calculations of several authors. The effect of meson exchange currents (MEC) were included in all the calculations considered here, either through the use of Siegert's theorem¹⁹ or by explicit consideration of these effects. MEC modify the interaction between the electromagnetic field of the photon and the deuterium nucleus. This modification is manifested by the introduction of many-body terms into the charge and current density operators and a consequent modification of the transition amplitudes between the initial state (which includes a photon and a deuterium nucleus in its ground state) and the final state (of the separated neutron and proton). According to Arenhövel,¹⁸ MEC effects may contribute as much as 25% to the ${}^2H(\gamma, n)$ cross section at 10 MeV, mostly through the electric transitions. Based on charge conservation, Siegert's theorem enables the calculation of these effects, for $E < 50$ MeV, as a function of the charge density operator alone, without explicit considera-

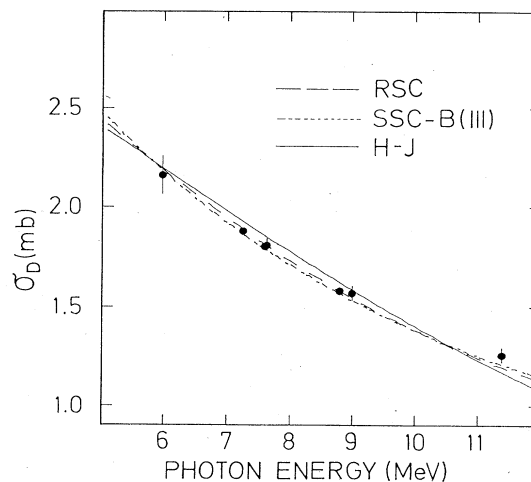


FIG. 4. Measured absolute photodisintegration cross section σ_D . The solid line represents the calculations of Partovi (Ref. 12) with no MEC, the dotted line is the result of Rustgi (Ref. 6) with MEC, while the dashed line is the result of Arenhövel (Ref. 7) obtained using the RSC potential.

tion of the nuclear current density operator. Most calculations also employ Siegert's hypothesis¹⁹ according to which interaction effects do not introduce many-body terms into the charge density operator. Table III summarizes the comparison between the present results and theory. In the following we give some comments regarding the calculations in the table.

First the Partovi cross sections were obtained using the Hamada-Johnston potential and employing Siegert's theorem and hypothesis. In the column labeled Feshbach-Lomon,¹⁷ results are given for the boundary condition model with two assumed values of the deuteron D -state probability (4.6% and 7.52%). In this model, a critical radius r_c is chosen; for $r > r_c$, a local nuclear potential is assumed, and for $r < r_c$ the interaction is approximated by boundary conditions at r_c . Here also Siegert's theorem and hypothesis were used. The next three columns show the results of Rustgi *et al.*⁶ with the

TABLE III. Measured and calculated values of the total photodisintegration cross section σ_D of the deuteron.

E (MeV)	Experiment (μb)	Partovi ^a	Feshbach-Lomon ^b		Predicted (μb)			Arenhövel ^d	
			$P_D = 4.6\%$	7.52%	SSC-B(I)	Rustgi <i>et al.</i> ^c Yale I	SSC-B (III)	RSC	Paris
5.97	2162±99	2201	2201	2180	2161	2173	2172	2192	2226
7.25	1882±11	1937	1935	1917	1855	1842	1871	1889	1919
7.60	1803±16	1865	1863	1844	1783	1764	1797	1815	1843
7.64	1810±28	1857	1855	1836	1774	1756	1789	1807	1835
8.80	1586±11	1617	1613	1595	1556	1526	1570	1580	1603
9.00	1570±36	1576	1571	1555	1522	1490	1535	1543	1565
11.39	1257±36	1186	1184	1172	1181	1143	1193	1192	1209
χ^2		55	52	26	18	68	7.9	5.2	23

^aReference 12.

^bReference 17.

^cReference 6.

^dReference 7.

Yale potential and with the super soft core potential, version B (SSC-B). In these calculations and in those of Arenhövel, no use was made of Siegert's theorem; the nuclear current density operator was calculated explicitly and Siegert's hypothesis was employed. The third column of calculations by Rustgi *et al.* lists the results for the SSC-B potential in approximation III where Siegert's hypothesis was relaxed, and exchange effects due to π , ρ , and ω mesons on both the charge and current density operators were included. Finally, the last two columns show the results of Arenhövel^{7,18} using the Reid soft core (RSC) and the Paris potentials, with an explicit calculation of MEC effects.

A comparison of the results of Table III leads to the following conclusions: (1) Apart from Rustgi's results using the Yale potential, there is, in general, a very good agreement (to within 5%) between the calculations and our measured values. (2) At $E < 12$ MeV, the differences between the explicit calculation of MEC and the use of Siegert's theorem are quite small. (3) The effect of including MEC contributions on the resulting σ_D in the energy range 6–12 MeV is small and of the same order of magni-

tude as that obtained using different potentials. (4) Considering the χ^2 values at the bottom of Table III, we can claim with 98% confidence that only the soft core potentials, SSC-B and RSC, with meson exchange included, yield an acceptable description of the experimental data.

Finally, it should be noted that the present new data can be combined with previous lower and higher energy data¹ to deduce the value of the electric polarizability α_D of the deuteron as was done in a recent paper.²⁰ This is because α_D is strongly related to the inverse-square energy-weighted photonuclear sum rule, and the energy weighting greatly enhances the contribution of the low energy data. It turns out that apart from the data point at 11.34 MeV, the values of σ_D used by the above authors are in excellent agreement with our values. Thus, our data essentially confirm the deduced value of α_D .

We would like to thank Prof. Arenhövel and Prof. Rustgi for sending us results of their calculations pertinent to our photon energies. Thanks are also due to Prof. Lomon for sending us his computer codes.

¹E. G. Fuller and H. Gerstenberg, National Bureau of Standards Report NBSIR 83-2742, 1984.

²M. P. DePascale *et al.*, Phys. Lett. **119B**, 30 (1982).

³A. Whetstone and J. Halpern, Phys. Rev. **109**, 2072 (1958).

⁴J. A. Phillips, J. S. Lawson, Jr., and P. G. Kruger, Phys. Rev. **80**, 326 (1950).

⁵C. A. Barnes, J. H. Carver, G. H. Stafford, and D. H. Wilkinson, Phys. Rev. **86**, 359 (1952).

⁶M. L. Rustgi, R. Vyas, and O. P. Rustgi, Phys. Rev. C **29**, 785 (1984), and private communication.

⁷H. Arenhövel, Nuovo Cimento **76A**, 256 (1983), and private communication.

⁸O. Y. Mafra, S. Kuniyoshi, and J. Goldemberg, Nucl. Phys. **A186**, 110 (1972).

⁹J. Ahrens *et al.*, Phys. Lett. **52B**, 49 (1974).

¹⁰J. E. E. Baglin, R. W. Carr, E. J. Bentz, and C. P. Wu, Nucl. Phys. **A201**, 593 (1973).

¹¹B. Weissman and H. L. Schultz, Nucl. Phys. **A174**, 129 (1971).

¹²F. Partovi, Ann. Phys. (N.Y.) **27**, 79 (1964).

¹³R. Moreh, S. Shlomo, and A. Wolf, Phys. Rev. C **2**, 1144 (1970).

¹⁴G. A. Bartholomew *et al.*, Nucl. Data **3A**, 367 (1967).

¹⁵R. Moreh and T. Bar-Noy, Nucl. Instrum. Methods **105**, 557 (1972).

¹⁶J. H. Hubble, Int. J. Appl. Radiat. Isot. **33**, 1269 (1982).

¹⁷E. L. Lomon and H. Feshbach, Ann. Phys. (N.Y.) **49**, 94 (1968).

¹⁸H. Arenhövel, in *Intermediate Energy Nuclear Physics*, edited by R. Bergere and C. Schaerf (World-Scientific, Singapore, 1982), p. 103.

¹⁹A. J. F. Siegert, Phys. Rev. **52**, 787 (1937).

²⁰J. L. Friar, S. Fallieros, and E. G. Fuller, Phys. Rev. C **27**, 1364 (1983); E. G. Fuller, private communication.